

Synthesis, crystal structure and properties of rubidium dihydrogencyanomelaminat semihydrate $\text{Rb}[\text{H}_2\text{C}_6\text{N}_9] \cdot \frac{1}{2} \text{H}_2\text{O}$

Barbara Jürgens, Henning A. Höpfe, Wolfgang Schnick

Angaben zur Veröffentlichung / Publication details:

Jürgens, Barbara, Henning A. Höpfe, and Wolfgang Schnick. 2004. "Synthesis, crystal structure and properties of rubidium dihydrogencyanomelaminat semihydrate $\text{Rb}[\text{H}_2\text{C}_6\text{N}_9] \cdot \frac{1}{2} \text{H}_2\text{O}$." *Zeitschrift für anorganische und allgemeine Chemie* 630 (1): 35–40. <https://doi.org/10.1002/zaac.200300164>.



Synthesis, Crystal Structure and Properties of Rubidium Dihydrogenicyanomelaminat Semihydrate $\text{Rb}[\text{H}_2\text{C}_6\text{N}_9] \cdot \frac{1}{2} \text{H}_2\text{O}$

Barbara Jürgens, Henning A. Höppe¹⁾, and Wolfgang Schnick*

München, Department Chemie der Ludwig-Maximilians-Universität

Dedicated to Professor Klaus-Jürgen Range on the Occasion of his 65th Birthday

Abstract. Rubidium dihydrogenicyanomelaminat semihydrate $\text{Rb}[\text{H}_2\text{C}_6\text{N}_9] \cdot \frac{1}{2} \text{H}_2\text{O}$ was obtained as colorless rod-like single crystals from a solution of $\text{Rb}_3[\text{C}_6\text{N}_9] \cdot \text{H}_2\text{O}$ and 0.1 M HCl after water evaporation at room temperature. According to the X-ray single-crystal structure determination ($\text{Rb}[\text{H}_2\text{C}_6\text{N}_9] \cdot \frac{1}{2} \text{H}_2\text{O}$: $C2/c$ (no. 15), $a = 2007.4(3)$ pm, $b = 512.2(1)$ pm, $c = 2168.0(4)$ pm, $\beta = 111.66(2)^\circ$, $Z = 8$, $R1 = 0.059$, 2391 independent reflections, 159 parameters) Rb^+ and cyclic planar $[\text{H}_2\text{C}_6\text{N}_9]^-$ ions as well as hydrate water molecules occur in the crystal. $\text{Rb}[\text{H}_2\text{C}_6\text{N}_9] \cdot \frac{1}{2} \text{H}_2\text{O}$

was investigated by FTIR and Raman spectroscopy, TG measurements and temperature-dependent X-ray powder diffraction. According to the thermoanalytic investigations, dehydration of $\text{Rb}[\text{H}_2\text{C}_6\text{N}_9] \cdot \frac{1}{2} \text{H}_2\text{O}$ starts above 60°C and is finished below 250°C .

Keywords: Carbon(IV) nitrides, Hydrogen bonds, Hydrate, Nitrido-carbonate(IV), Vibrational Spectroscopy

Synthese, Kristallstruktur und Eigenschaften von Rubidium-dihydrogenicyanomelaminat-Semihydrat $\text{Rb}[\text{H}_2\text{C}_6\text{N}_9] \cdot \frac{1}{2} \text{H}_2\text{O}$

Inhaltsübersicht. Rubidium-dihydrogenicyanomelaminat-Semihydrat $\text{Rb}[\text{H}_2\text{C}_6\text{N}_9] \cdot \frac{1}{2} \text{H}_2\text{O}$ wurde in Form farbloser stäbchenförmiger Kristalle durch Mischen einer Lösung von $\text{Rb}_3[\text{C}_6\text{N}_9] \cdot \text{H}_2\text{O}$ mit 0,1 M HCl und anschließendes Verdunsten des Lösungsmittels bei Raumtemperatur erhalten. Nach der Einkristallstrukturanalyse ($\text{Rb}[\text{H}_2\text{C}_6\text{N}_9] \cdot \frac{1}{2} \text{H}_2\text{O}$: $C2/c$ (Nr. 15), $a = 2007,4(3)$ pm, $b = 512,2(1)$ pm, $c = 2168,0(4)$ pm, $\beta = 111,66(2)^\circ$, $Z = 8$, $R1 = 0,059$,

2391 unabhängige Reflexe, 159 Parameter) liegen im Festkörper Rb^+ - und cyclische $[\text{H}_2\text{C}_6\text{N}_9]^-$ -Ionen sowie Kristallwasser-Moleküle vor. $\text{Rb}[\text{H}_2\text{C}_6\text{N}_9] \cdot \frac{1}{2} \text{H}_2\text{O}$ wurde mittels FTIR und Raman-Spektroskopie, TG-Messungen sowie temperaturabhängiger Pulver-Röntgenbeugung charakterisiert. Nach den thermoanalytischen Untersuchungen setzt die Dehydratation von $\text{Rb}[\text{H}_2\text{C}_6\text{N}_9] \cdot \frac{1}{2} \text{H}_2\text{O}$ bei 60°C ein und ist bis 250°C abgeschlossen.

1 Introduction

Alkali, alkaline earth, and transition metal dicyanamides intensively have been studied during the last few years [1–14]. From a formal point of view, these compounds may be regarded as nitridocarbonates(IV), and therefore they derive from postulated binary carbon nitride C_3N_4 . Because of their triple bonds the bent dicyanamide ions $[\text{N}(\text{CN})_2]^-$ are suitable for oligomerization and polymerization reactions leading to extended C-N species. Thermolysis reactions of the dicyanamides $\text{M}^{\text{II}}[\text{N}(\text{CN})_2]_2$ with $\text{M}^{\text{II}} = \text{Mg}$, Ca, Sr, Ba or Pb lead to amorphous products containing undefined polymeric C-N anions [1, 2]. For the alkali dicy-

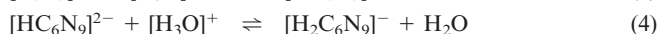
anamides $\text{M}^{\text{I}}[\text{N}(\text{CN})_2]$ with $\text{M}^{\text{I}} = \text{Na}$, K, Rb trimerization of the anions and formation of cyclic tricyanomelaminat ions $[\text{C}_6\text{N}_9]^{3-}$ was observed [5–7]. The crystal structures of both the anhydrous alkali tricyanomelaminates $\text{M}^{\text{I}}_3[\text{C}_6\text{N}_9]$ ($\text{M}^{\text{I}} = \text{Na}$, K, Rb) and the respective hydrates $\text{Na}_3[\text{C}_6\text{N}_9] \cdot 3 \text{H}_2\text{O}$ and $\text{M}^{\text{I}}_3[\text{C}_6\text{N}_9] \cdot \text{H}_2\text{O}$ ($\text{M}^{\text{I}} = \text{K}$, Rb) thoroughly have been characterized [4, 7, 11]. Furthermore, the thermal behavior of $\text{Li}[\text{N}(\text{CN})_2]$ and $\text{Cs}[\text{N}(\text{CN})_2]$ was investigated, however a structure determination of the postulated tricyanomelaminates $\text{M}^{\text{I}}_3[\text{C}_6\text{N}_9]$ ($\text{M}^{\text{I}} = \text{Li}$, Cs) was not possible as yet [12–14].

The postulated free acids dicyanamide $\text{HN}(\text{CN})_2$ and its trimer tricyanomelaminat $\text{H}_3\text{C}_6\text{N}_9$ are of considerable interest because they exhibit a high potential as precursor compounds for the synthesis of binary carbon(IV) nitride C_3N_4 (eq. (1) and (2)). According to the literature, these acids can not be isolated due to polymerization in aqueous solution [15, 16]. Tricyanomelaminates $\text{M}^{\text{I}}_3[\text{C}_6\text{N}_9]$ in contrast to dicyanamides exhibit an alkaline reaction when dissolved in water (eq. (3)-(5)). The free acid $\text{H}_3\text{C}_6\text{N}_9$ is assumed to be less strong as compared with $\text{HN}(\text{CN})_2$. Therefore the synthesis of tricyanomelaminat seems to be easier than the isolation of dicyanamide $\text{HN}(\text{CN})_2$. In order to understand

* Prof. Dr. W. Schnick
Department Chemie der Ludwig-Maximilians-Universität
Butenandtstraße 5-13 (D)
D-81377 München, Germany
Fax: +49-89-2180-77440
E-mail: wolfgang.schnick@uni-muenchen.de

¹⁾ New address: Inorganic Chemistry Laboratory, South Parks Road, Oxford, OX1 3QR, UK

the acid-base system $[\text{C}_6\text{N}_9]^{3-} / [\text{HC}_6\text{N}_9]^{2-} / [\text{H}_2\text{C}_6\text{N}_9]^- / \text{H}_3\text{C}_6\text{N}_9$ and with the further aim to synthesize the free acid tricyanomelamine detailed knowledge of the syntheses and properties of the mono- and diprotonated species $[\text{HC}_6\text{N}_9]^{2-}$ and $[\text{H}_2\text{C}_6\text{N}_9]^-$ is of considerable interest. In the past only a very few protonated tricyanomelaminates have been described in the literature: The hydrogentricyanomelaminates $\text{M}^{\text{II}}[\text{HC}_6\text{N}_9] \cdot 3 \text{H}_2\text{O}$ with $\text{M}^{\text{II}} = \text{Co}, \text{Ni}, \text{Cu}$ or Cd [17] and the dihydrogentricyanomelaminates $\{\text{Co}[\text{H}_2\text{C}_6\text{N}_9]_2(\text{H}_2\text{O})_4\} \cdot 6 \text{H}_2\text{O}$ [18] were synthesized by acidifying solutions of $\text{Na}_3[\text{C}_6\text{N}_9] \cdot 3 \text{H}_2\text{O}$.



With respect to the differing behavior of dicyanamides of monovalent and divalent metals, respectively, as mentioned above and the possible redox reactivity of transition metals, we chose alkali tricyanomelaminates for our investigations. Herein we report about the synthesis, crystal structure, and properties of the dihydrogentricyanomelaminates $\text{Rb}[\text{H}_2\text{C}_6\text{N}_9] \cdot \frac{1}{2} \text{H}_2\text{O}$.

2 Experimental Part

Synthesis and thermal properties

An amount of 1.05 ml HCl (0.1 M) was added to a solution of 25.0 mg (0.053 mmol) $\text{Rb}_3[\text{C}_6\text{N}_9] \cdot \text{H}_2\text{O}$ in 20 ml H_2O . At room temperature the water was evaporated within a few days and colorless rod-like crystals of $\text{Rb}[\text{H}_2\text{C}_6\text{N}_9] \cdot \frac{1}{2} \text{H}_2\text{O}$ were formed. The starting material $\text{Rb}_3[\text{C}_6\text{N}_9] \cdot \text{H}_2\text{O}$ was obtained from $\text{Na}_3[\text{C}_6\text{N}_9]$ and RbCl (Alfa Aesar, 99 %) through ion exchange in aqueous solution and subsequent cooling; for details about the syntheses of $\text{Rb}_3[\text{C}_6\text{N}_9] \cdot \text{H}_2\text{O}$ and $\text{Na}_3[\text{C}_6\text{N}_9]$ see ref. [11] and [5], respectively. In order to investigate the thermal behavior, samples of $\text{Rb}[\text{H}_2\text{C}_6\text{N}_9] \cdot \frac{1}{2} \text{H}_2\text{O}$ were filled into alumina crucibles which were heated in glass ampoules under argon atmosphere to different temperatures between 100 °C and 400 °C. White (100 °C, 200 °C) and beige-brown (300 °C, 400 °C) powders, respectively, were obtained after cooling to room temperature. These products were characterized by both powder diffraction and FTIR spectroscopy. Additionally, thermogravimetric investigations were performed on a TGA 92 (Setaram).

X-Ray Diffraction

X-ray diffraction data of a $\text{Rb}[\text{H}_2\text{C}_6\text{N}_9] \cdot \frac{1}{2} \text{H}_2\text{O}$ single-crystal were collected on a four-circle diffractometer (STOE Stadi 4) using $\text{Mo-K}\alpha$ radiation. According to the observed extinctions of the monoclinic lattice, the space groups $C2/c$ and Cc were considered. The structure solution and refinement was possible only in $C2/c$ (no.15). The crystal structure of $\text{Rb}[\text{H}_2\text{C}_6\text{N}_9] \cdot \frac{1}{2} \text{H}_2\text{O}$ was solved using direct methods with the program SHELXTL [19]. The structure model was refined with anisotropic displacement parameters for all non H-atoms. The positions of all hydrogen atoms unequivo-

Table 1 Crystallographic Data for $\text{Rb}[\text{H}_2\text{C}_6\text{N}_9] \cdot \frac{1}{2} \text{H}_2\text{O}$.

formula	$\text{Rb}[\text{H}_2\text{C}_6\text{N}_9] \cdot \frac{1}{2} \text{H}_2\text{O}$	
$M_w / \text{g} \cdot \text{mol}^{-1}$	294.65	
crystal system	monoclinic	
space group	$C2/c$ (no. 15)	
T / K	293(2)	293(2)
diffractometer	STOE Stadi 4 (single-crystal)	STOE Stadi P (powder)
radiation (λ / pm)	$\text{Mo-K}\alpha$ (71.073; graphite monochromator)	$\text{Cu-K}\alpha_1$ (154.06; Ge(111)-monochromator)
a / pm	2007.4(3)	2008.27(3)
b / pm	512.2(1)	512.62(1)
c / pm	2168.0(4)	2168.93(3)
$\beta / ^\circ$	111.66(2)	111.650(1)
$V / 10^6 \text{pm}^3$	2071.8(6)	2075.34(6)
program	SHELXTL (Version 5.10) [19]	GSAS [21]
Z	8	
$\rho_{\text{calcd}} / \text{g} \cdot \text{cm}^{-3}$	1.889	
F(000)	1144	
μ / mm^{-1}	4.774	
crystal size / mm^3	0.51 x 0.24 x 0.17	
diffraction range	$4.04^\circ \leq 2\theta \leq 55.00^\circ$	
index range	$-26 \leq h \leq 26, -6 \leq k \leq 6, -28 \leq l \leq 28$	
scan type	ω scan	
total no. reflections	9564	
independent reflections	2391	
observed reflections	1844 ($R_{\text{int}} = 0.0623$) with ($F_o^2 \geq 2\sigma F_o^2$)	
refined parameters	159	
corrections	absorption, extinction, Lorentz, polarization numerical (ω scans)	
absorption correction	numerical (ω scans)	
min./max. transmission ratio	0.3696 / 0.5171	
min./max. residual electron density / $\text{e}\text{\AA}^{-3}$	-0.43 / 0.33	
extinction coefficient χ	0.0012(2)	
GOF	1.085	
R indices (all data)	$R1 = 0.0592$ $wR2 = 0.0832$ with $w = [\sigma^2(F_o^2) + (0.0354 P)^2 + 1.6513 P]^{-1}$ where $P = (F_o^2 + 2 F_c^2) / 3$	

cally could be determined from difference Fourier syntheses. The determined atomic positions represent local maxima of the electron density distribution. For light atoms (especially H) the refined positions usually do not coincide with the real atomic sites. Consequently, atomic distances N-H or O-H are obtained, which are unreasonably short. Therefore, idealized positions for the H atoms have been chosen, which lead to bond lengths N-H near 100 pm [20]. The position of the hydrogen atom of the crystal water molecule was refined using a riding model. Details of the structure determination and the crystallographic data are summarized in Table 1. The atomic coordinates and displacement parameters are given in Tables 2 and 3. Interatomic distances and angles are listed in Table 4.

All reflections detected by X-ray powder diffractometry (STOE Stadi P) of $\text{Rb}[\text{H}_2\text{C}_6\text{N}_9] \cdot \frac{1}{2} \text{H}_2\text{O}$ have been indexed and their observed intensities agree well with the calculated diffraction pattern based on the single-crystal X-ray diffraction data. Additionally, the lattice parameters were refined (Table 1) using the program GSAS [21]. Further details of the crystal structure investigation reported in this paper may be obtained from the Fachinformationszentrum Karlsruhe, D-76344 Eggenstein-Leopoldshafen, Germany (fax: (+49)7247-808-666, E-mail: crysdata@fiz-karlsruhe.de), by quoting the depository number CSD-413139.

Table 2 Atomic coordinates and displacement factors (in pm²) of Rb[H₂C₆N₉] · 1/2 H₂O. U_{eq} is defined as one third of the trace of the orthogonalized U_{ij} tensor.

atom	Wyckoff position	x	y	z	U_{eq}
Rb	8f	0.40628(2)	0.35430(7)	0.28315(2)	0.0369(2)
C1	8f	0.1387(2)	0.3462(7)	0.0144(2)	0.0281(6)
C2	8f	0.2112(2)	0.1222(6)	0.1125(2)	0.0262(6)
C3	8f	0.2616(2)	0.4492(7)	0.0737(2)	0.0263(6)
C4	8f	0.0204(2)	0.2790(8)	-0.0484(2)	0.0354(8)
C5	8f	0.2721(2)	-0.1075(6)	0.2036(2)	0.0313(7)
C6	8f	0.3779(2)	0.5766(7)	0.1207(2)	0.0314(7)
N1	8f	0.1464(2)	0.1613(6)	0.0605(2)	0.030(6)
H11	8f	0.111(2)	0.067(7)	0.059(2)	0.04(1)
N2	8f	0.2686(2)	0.2699(5)	0.1196(2)	0.0272(6)
N3	8f	0.1978(2)	0.4891(6)	0.0217(2)	0.0287(6)
H31	8f	0.194(2)	0.599(6)	-0.006(2)	0.018(8)
N4	8f	0.0812(2)	0.4036(6)	-0.0366(2)	0.0345(7)
N5	8f	0.2110(2)	-0.0719(6)	0.1522(2)	0.0318(6)
N6	8f	0.3139(2)	0.6059(6)	0.0720(2)	0.0314(6)
N7	8f	-0.0352(2)	0.1867(8)	-0.0641(2)	0.0518(9)
N8	8f	0.3218(2)	-0.1536(6)	0.2501(2)	0.0456(7)
N9	8f	0.4348(2)	0.5657(7)	0.1598(2)	0.0444(8)
OW	4e	0	0.5016(8)	1/4	0.055(2)
HW	8f	0.02350	0.3764	0.2866	0.067

Table 3 Anisotropic displacement factors (in pm²) for Rb[H₂C₆N₉] · 1/2 H₂O, given as $\exp[-2\pi^2(U_{11}h^2a^{*2} + \dots + 2U_{13}hla^*c^*)]$.

atom	U_{11}	U_{22}	U_{33}	U_{23}	U_{13}	U_{12}
Rb	333(18)	420(2)	363(2)	27(2)	138(2)	33(2)
C1	239(13)	343(17)	259(14)	-8(14)	90(11)	-37(14)
C2	242(13)	302(17)	248(14)	-24(14)	97(11)	-25(14)
C3	220(13)	309(16)	249(14)	-12(14)	75(12)	-36(13)
C4	289(17)	480(20)	251(15)	68(16)	52(13)	-61(16)
C5	290(15)	269(18)	391(17)	59(15)	137(14)	-33(14)
C6	319(16)	335(18)	312(16)	56(14)	146(14)	-36(14)
N1	229(12)	375(16)	282(13)	41(13)	78(10)	-70(13)
N2	226(12)	305(14)	279(13)	34(12)	88(10)	-33(11)
N3	212(12)	332(15)	278(13)	56(12)	46(10)	-75(12)
N4	245(12)	412(18)	332(14)	55(13)	51(11)	-63(12)
N5	283(13)	327(16)	337(14)	59(12)	106(11)	-41(12)
N6	223(12)	404(17)	271(12)	86(12)	40(10)	-50(12)
N7	296(15)	790(30)	390(16)	92(18)	37(12)	-167(17)
N8	376(15)	393(18)	522(18)	141(16)	77(14)	6(15)
N9	262(14)	600(20)	408(17)	85(16)	53(13)	-45(15)
OW	510(20)	400(20)	750(30)	0	220(30)	0

Table 4 Interatomic distances (in pm) and angles (in °) in Rb[H₂C₆N₉] · 1/2 H₂O.

C1–N1	134.2(4)	N1–C1–N3	115.7(3)	Rb–N2	363.0(3)
C1–N3	135.0(4)	N1–C1–N4	127.9(3)	Rb–N5	317.6(3)
C1–N4	130.4(4)	N1–C2–N2	121.2(3)	Rb–N7	308.5(3)
C2–N1	138.5(4)	N1–C2–N5	114.5(3)	Rb–N8	297.4(3)
C2–N2	133.9(4)	N2–C2–N5	124.3(3)		304.4(3)
C2–N5	131.6(4)	N2–C3–N3	121.6(3)	Rb–N9	312.7(3)
C3–N2	132.2(4)	N2–C3–N6	125.0(3)		315.6(3)
C3–N3	137.1(4)	N3–C1–N4	116.4(3)	Rb–OW	288.7(3) (2x)
C3–N6	133.2(4)	N3–C3–N6	113.4(3)		
C4–N4	131.6(4)	N4–C4–N7	173.1(4)		
C4–N7	114.2(4)	N5–C5–N8	174.1(3)	C1–N1–H11	120(2)
C5–N5	132.9(4)	N6–C6–N9	174.5(3)	C2–N1–H11	118(2)
C5–N8	115.2(4)	C1–N1–C2	121.8(3)	C1–N3–H31	116(2)
C6–N6	133.6(4)	C2–N2–C3	117.4(2)	C3–N3–H31	121(2)
C6–N9	114.6(4)	C1–N3–C3	122.3(3)		
N1–H11	99(1)	C1–N4–C4	121.5(3)		
N3–H31	99(1)	C2–N5–C5	115.3(3)		
		C3–N6–C6	116.6(3)		

In order to investigate the thermal behavior of Rb[H₂C₆N₉] · 1/2 H₂O temperature-dependent X-ray powder diffraction patterns were recorded on a STOE Stadi P powder diffractometer (Mo-K α_1) with a computer-controlled STOE furnace between room temperature and 400 °C.

Vibrational Spectroscopic Investigations

FTIR spectra were recorded on a Bruker IFS 66v/S spectrometer scanning a range from 400 cm⁻¹ to 4000 cm⁻¹. The samples were thoroughly mixed with dried KBr (5 mg sample, 500 mg KBr). FT-Raman spectra were excited by a Bruker FRA 106/S module with a Nd-YAG laser ($\lambda = 1064$ nm) scanning a range from 10 cm⁻¹ up to 3500 cm⁻¹. All preparation procedures have been performed in a glove box under an atmosphere of purified argon.

3 Results and Discussion

Crystal Structure

In the solid Rb[H₂C₆N₉] · 1/2 H₂O is built up from Rb⁺ and dihydrogenicyanomelamine ions [H₂C₆N₉]⁻ as well as crystal water molecules (Fig. 1). The nearly planar [H₂C₆N₉]⁻ ions form two types of layers which are tilted to each other by an angle of 82.6(5)° (Fig. 2). The water molecules are situated between these layers. All 17 atoms of the anion are nearly coplanar corresponding to the molecular symmetry C_s, however the crystallographic point symmetry of the complex anion is only C₁. The conformation of the three N=C=N groups forming the side-arms of the *s*-triazine ring system are arranged in a manner breaking a possible threefold symmetry of the entire anion: The two arms N5–C5–N8 and N6–C6–N9 are arranged nearly parallel to each other (Fig. 3). The same situation is found in {Co[H₂C₆N₉]₂(H₂O)₄} · 6 H₂O [18], M[HC₆N₉] · 3 H₂O (M = Co, Ni, Cu, Cd) [17], M₃[C₆N₉] · H₂O (M = K, Rb) [11] and also in the anhydrous tricyanomelaminates M₃[C₆N₉] (M = Na, K, Rb) [5, 6]. Contrarily, a threefold symmetry of the anion [C₆N₉]³⁻ occurs in Na₃[C₆N₉] · 3 H₂O [4, 7].

The hydrogen atoms H11 and H31 are bound to N1 and N3, respectively. Only the atom N2, which is situated between the side-arms N6–C6–N9 and N5–C5–N8, carries no proton (Fig. 3). With respect to this protonation the ring nitrogen atoms may be considered to be the most basic ones of the complex anion. Equally, in the other known dihydrogenicyanomelamine {Co[H₂C₆N₉]₂(H₂O)₄} · 6 H₂O protonation of the ring N atoms and not of the side-arms is observed [18].

Each Rb⁺ ion is surrounded by one O atom of the crystal water and seven N atoms. The latter ones belong to five different [H₂C₆N₉]⁻ ions. Predominantly, the terminal nitrogen atoms N7, N8 (2x) and N9 (2x) contribute to the coordination of the alkali cations, while only one ring atom (N2) and one bridging atom (N5) are involved in the coordination sphere of Rb⁺.

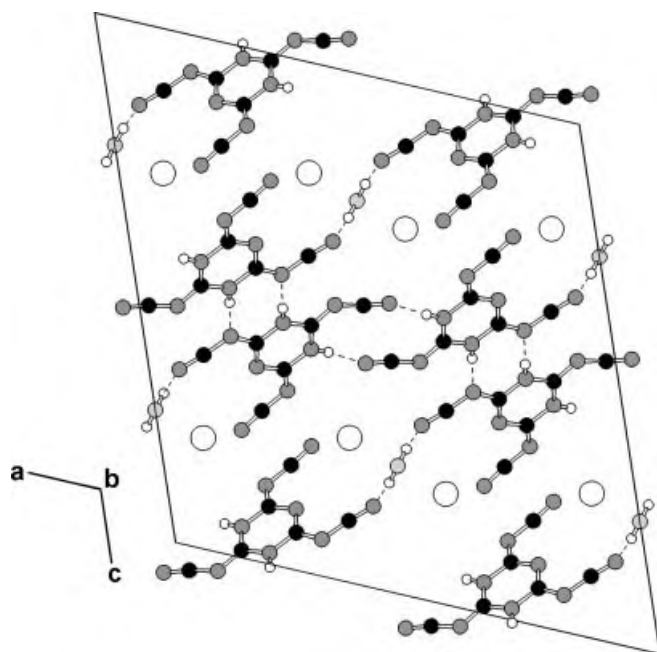


Fig. 1 Crystal structure of $\text{Rb}[\text{H}_2\text{C}_6\text{N}_9] \cdot \frac{1}{2} \text{H}_2\text{O}$ (view along [010]; Rb: large open circles, C: black circles, N and O: gray circles, H: small open circles). The hydrogen bonds are shown as broken lines.

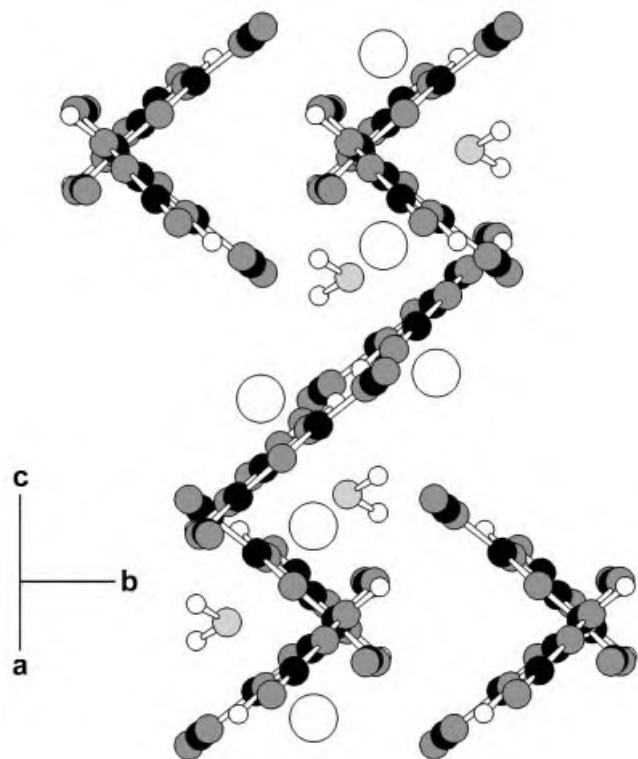


Fig. 2 Sheets within the crystal structure of $\text{Rb}[\text{H}_2\text{C}_6\text{N}_9] \cdot \frac{1}{2} \text{H}_2\text{O}$ (view along [010]; Rb: large open circles, C: black circles, N and O, gray circles, H: small open circles). The angle between two $[\text{H}_2\text{C}_6\text{N}_9]^-$ layers is $82.6(5)^\circ$.

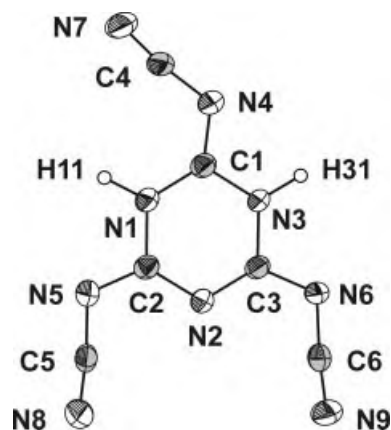


Fig. 3 Dihydrogen-tricyanomelaminates ions $[\text{H}_2\text{C}_6\text{N}_9]^-$ in $\text{Rb}[\text{H}_2\text{C}_6\text{N}_9] \cdot \frac{1}{2} \text{H}_2\text{O}$, displacement ellipsoids are shown at the 50% probability level.

In the crystal structure of $\text{Rb}[\text{H}_2\text{C}_6\text{N}_9] \cdot \frac{1}{2} \text{H}_2\text{O}$ intermolecular hydrogen bonds between the protonated ring atoms and the terminal nitrogen atoms are observed, thus forming pairs of tricyanomelaminates ions (Fig. 1). Further hydrogen bonds have been detected between the crystal water molecule and the terminal nitrogen N9. The parameters of the hydrogen bonds $\text{N}7 \cdots \text{H}11 - \text{N}1$ (distance $\text{N}7 \cdots \text{N}1$: 288 pm, angle $\text{N}7 \cdots \text{H}11 - \text{N}1$: 173°), $\text{N}6 \cdots \text{H}31 - \text{N}3$ (distance $\text{N}6 \cdots \text{N}3$: 285 pm, angle $\text{N}6 \cdots \text{H}31 - \text{N}3$: 177°) and $\text{N}9 \cdots \text{HW} - \text{OW}$ (distance $\text{N}9 \cdots \text{OW}$: 294 pm, angle $\text{N}9 \cdots \text{HW} - \text{OW}$: 165°) are in good agreement with the values found for other medium strong hydrogen bonds $\text{N} \cdots \text{H} - \text{X}$ ($\text{X} = \text{O}, \text{N}$) [22, 23].

The distances C–N range from 130 to 139 pm, except those of the terminal nitrogen atoms (114 – 115 pm), the latter ones representing triple bonds. The angles within the $\text{N}=\text{C}=\text{N}$ side-arms are almost linear ($173 - 174^\circ$). The respective values are comparable to those found for the dihydrogen-tricyanomelaminates ion in $\{\text{Co}[\text{H}_2\text{C}_6\text{N}_9]_2(\text{H}_2\text{O})_4\} \cdot 6 \text{H}_2\text{O}$ or in compounds, which are built up from $[\text{HC}_6\text{N}_9]^{2-}$ or $[\text{C}_6\text{N}_9]^{3-}$ ions (e. g. $\text{M}^{\text{II}}[\text{HC}_6\text{N}_9] \cdot 3 \text{H}_2\text{O}$ ($\text{M} = \text{Co}, \text{Ni}, \text{Cu}, \text{Cd}$), and $\text{Na}_3[\text{C}_6\text{N}_9] \cdot 3 \text{H}_2\text{O}$). The coordination distances $\text{Rb}^+ \cdots \text{N}$ are in the range 297 – 318 pm. This is comparable to the respective values observed in $\text{Rb}[\text{HCN}_2]$ (293 – 353 pm) [24] and $\text{Rb}_3[\text{C}_6\text{N}_9]$ (310 – 317 pm).

Vibrational Spectroscopy

The vibrational spectroscopic behavior of the dihydrogen-tricyanomelaminates ion $[\text{H}_2\text{C}_6\text{N}_9]^-$ is quite similar to that of the non-protonated tricyanomelaminates ion $[\text{C}_6\text{N}_9]^{3-}$. According to the formula $3 \cdot \text{N} - 6$ (N = number of atoms) 39 vibrations are expected for the $[\text{C}_6\text{N}_9]^{3-}$ ion. The assignment of these vibrations have been discussed in detail for $\text{Na}_3[\text{C}_6\text{N}_9]$ and $\text{Na}_3[\text{C}_6\text{N}_9] \cdot 3 \text{H}_2\text{O}$ [7]. For the dihydrogen-tricyanomelaminates ion $[\text{H}_2\text{C}_6\text{N}_9]^-$ further six vi-

brations may occur. Because of the protonation of its *s*-triazine ring a threefold molecular symmetry is impossible. Its symmetry is reduced to C_1 which is confirmed by the crystal structure determination of $\text{Rb}[\text{H}_2\text{C}_6\text{N}_9] \cdot \frac{1}{2} \text{H}_2\text{O}$ (Table 2).

In Fig. 4 the FTIR and FT-Raman spectra of $\text{Rb}[\text{H}_2\text{C}_6\text{N}_9] \cdot \frac{1}{2} \text{H}_2\text{O}$ are compared with the respective spectra of the non-protonated monohydrate $\text{Rb}_3[\text{C}_6\text{N}_9] \cdot \text{H}_2\text{O}$ [11]. The signal patterns of both compounds are very similar. In the case of $\text{Rb}[\text{H}_2\text{C}_6\text{N}_9] \cdot \frac{1}{2} \text{H}_2\text{O}$ more significant signals are observed in the region $3130 - 2600 \text{ cm}^{-1}$ (FTIR) as compared to the non-protonated compound. These may be assigned to the vibrations ν_{NH} (N-H \cdots N) of the dihydrogenicyanomelaminat ion. In the vibrational spectra of $\text{Rb}[\text{H}_2\text{C}_6\text{N}_9] \cdot \frac{1}{2} \text{H}_2\text{O}$ the vibrations $\nu_{\text{s}}\text{C}\equiv\text{N}$ and $\nu_{\text{as}}\text{C}\equiv\text{N}$ are observed at higher values (ca. 2200 cm^{-1}) than for $\text{Rb}_3[\text{C}_6\text{N}_9] \cdot \text{H}_2\text{O}$ (ca. 2160 cm^{-1}). In the region $1700 - 1460 \text{ cm}^{-1}$, which is mainly caused by the molecular vibrations of the complex anions, the spectra of both compounds differ significantly, as for $\text{Rb}[\text{H}_2\text{C}_6\text{N}_9] \cdot \frac{1}{2} \text{H}_2\text{O}$

more signals are found because of the H atoms bound to the *s*-triazine ring.

Thermal behavior

According to TG measurements, dehydration of $\text{Rb}[\text{H}_2\text{C}_6\text{N}_9] \cdot \frac{1}{2} \text{H}_2\text{O}$ starts above 60°C , and it is finished below 250°C . The X-ray powder pattern of a sample of $\text{Rb}[\text{H}_2\text{C}_6\text{N}_9] \cdot \frac{1}{2} \text{H}_2\text{O}$, which was heated up to 100°C , shows reflections of $\text{Rb}[\text{H}_2\text{C}_6\text{N}_9] \cdot \frac{1}{2} \text{H}_2\text{O}$ as well as a few, broad reflections of a new phase. After heating up to 200°C and subsequent cooling the reflections of the starting material all have disappeared and only reflections of the new phase were observed. At higher temperatures the samples become X-ray amorphous. According to IR spectroscopy the intermediate phase presumably is anhydrous $\text{Rb}[\text{H}_2\text{C}_6\text{N}_9]$.

$\text{Rb}[\text{H}_2\text{C}_6\text{N}_9] \cdot \frac{1}{2} \text{H}_2\text{O}$ is soluble in water where it reacts as an acid. Further investigations are planned to determine the $\text{pK}_{\text{a}} / \text{pK}_{\text{b}}$ values within the system $[\text{C}_6\text{N}_9]^{3-} / [\text{HC}_6\text{N}_9]^{2-} / [\text{H}_2\text{C}_6\text{N}_9]^-$.

Acknowledgments. The authors would like to thank *Sabine Schmid* (Department Chemie, LMU München) for performing the TG measurements and *Dr. Elisabeth Irran* (TU Berlin) for her help with the temperature-dependent X-ray powder diffraction measurements and the Rietveld refinement. Financial support from the Fonds der Chemischen Industrie and from the Deutsche Forschungsgemeinschaft is gratefully acknowledged.

References

- [1] B. Jürgens, E. Irran, W. Schnick, *J. Solid State Chem.* **2001**, 157, 241.
- [2] B. Jürgens, H. A. Höpfe, W. Schnick, *Solid State Sci.* **2002**, 4, 821.
- [3] W. Madelung, E. Kern, *Liebigs Ann. Chem.* **1922**, 427, 1.
- [4] J. L. Hoard, *J. Am. Chem. Soc.* **1938**, 80, 1194.
- [5] B. Jürgens, E. Irran, J. Schneider, W. Schnick, *Inorg. Chem.* **2000**, 39, 665.
- [6] E. Irran, B. Jürgens, W. Schnick, *Chem. Eur. J.* **2001**, 7, 5372.
- [7] B. Jürgens, W. Milius, P. Morys, W. Schnick, *Z. Anorg. Allg. Chem.* **1998**, 624, 91.
- [8] J. L. Manson, C. R. Kmety, Q.-Z. Huang, J. W. Lynn, G. M. Bendele, S. Pagola, P. W. Stephens, L. M. Liable-Sands, A. L. Rheingold, A. J. Epstein, J. S. Miller, *Chem. Mater.* **1998**, 10, 2552.
- [9] S. R. Batten, P. Jensen, B. Moubaraki, K. S. Murray, R. Robson, *Chem. Commun.* **1998**, 439.
- [10] M. Kurmoo, C. J. Kepert, *New. J. Chem.* **1998**, 2, 1515.
- [11] E. Irran, B. Jürgens, W. Schnick, *Solid State Sci.* **2002**, 4, 1305.
- [12] A. P. Purdy, E. Houser, C. F. George, *Polyhedron* **1997**, 16, 3671.
- [13] P. Starynowicz, *Acta Crystallogr.* **1991**, C47, 2198.
- [14] B. Jürgens, W. Schnick, unpublished results.
- [15] W. Madelung, E. Kern, *Liebigs Ann. Chem.* **1922**, 427, 26.
- [16] E. C. Franklin, *J. Am. Chem. Soc.* **1922**, 44, 486.

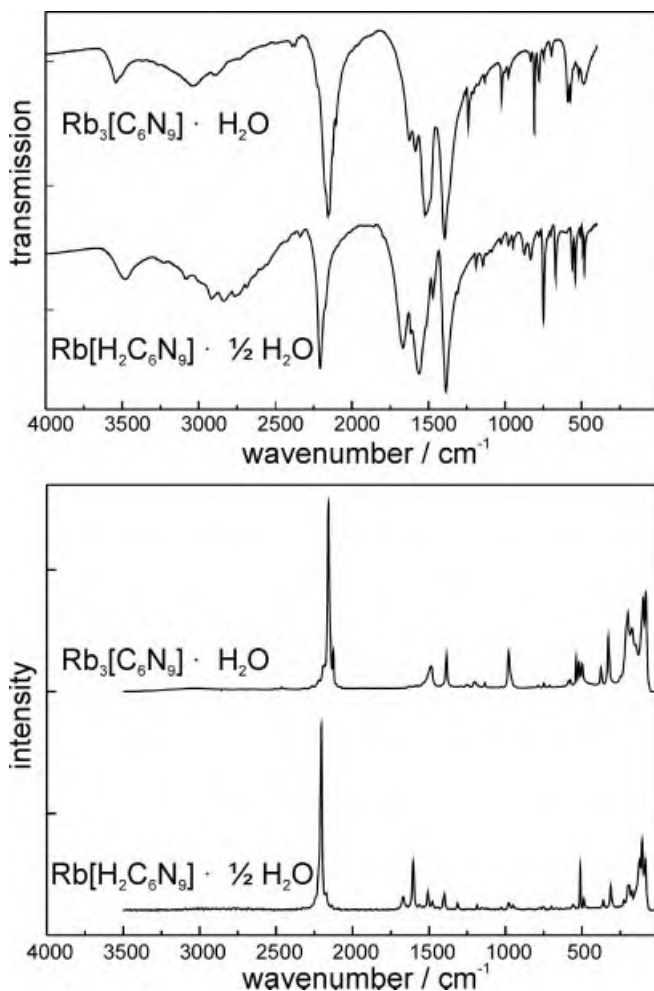


Fig. 4 FTIR- (top) and FT-Raman (bottom) spectra of $\text{Rb}[\text{H}_2\text{C}_6\text{N}_9] \cdot \frac{1}{2} \text{H}_2\text{O}$ in comparison to those of $\text{Rb}_3[\text{C}_6\text{N}_9] \cdot \text{H}_2\text{O}$ [11].

- [17] B. F. Abrahams, S. J. Egan, B. F. Hoskins, R. Robson, *Chem. Commun.* **1996**, 1099.
- [18] B. F. Abrahams, S. J. Egan, B. F. Hoskins, R. Robson, *Acta Crystallogr.* **1996**, C52, 2427.
- [19] G. M. Sheldrick, *SHELXTL, V 5.10 Crystallographic System*, Bruker AXS Analytical X-ray Instruments Inc., Madison, **1997**.
- [20] A. F. Wells, *Structural Inorganic Chemistry*, 5. Edition, Clarendon Press, Oxford, **1984**, p. 653.
- [21] A. C. Larson, R. B. von Dreele, **1990**, General Structure Analysis System, Los Alamos National Laboratory Report LAUR 86-748.
- [22] R. Steudel, *Chemie der Nichtmetalle*, 2. völlig neu bearbeitete Auflage, de Gruyter, Berlin and New York **1998**, p. 142 and p. 203.
- [23] T. Steiner, *Angew. Chem.* **2002**, 114, 50; *Angew. Chem. Int. Ed.* **2002**, 41, 48.
- [24] M. Becker, M. Jansen, *Z. Naturforsch.* **1999**, 54b, 1375.